JPET Fast Forward. Published on April 3, 2020 as DOI: 10.1124/jpet.119.261180
This article has not been copyedited and formatted. The final version may differ from this version.

JPET # 261180

The development and characterization of an scFv-Fc fusion based gene therapy to reduce the psychostimulant effects of methamphetamine abuse

Charles E. Hay[1], Laura E. Ewing[1], Michael D. Hambuchen[1], Shannon M. Zintner[2], Juliana C. Small[2], Chris T. Bolden[1], William E Fantegrossi[1], Paris Margaritis[2,3,4], S. Michael Owens[1], Eric C. Peterson[1].

[1]University of Arkansas for Medical Sciences, Little Rock, Arkansas, U.S.A.

[2]The Children's Hospital of Philadelphia, Philadelphia, Pennsylvania, U.S.A.

[3]The Raymond G. Perelman Center for Cellular and Molecular Therapeutics, The Children's Hospital of Philadelphia, Philadelphia, Pennsylvania, U.S.A.

[4]Department of Pediatrics, The University of Pennsylvania, Perelman School of Medicine, Philadelphia, Pennsylvania, U.S.A.

Running title: AAV-Scfv-Fc fusion therapy mitigates METH's stimulant effects

Corresponding author: Eric C. Peterson, PhD

University of Arkansas for Medical Sciences, Department of Pharmacology and Toxicology 4301 West Markham Street, Slot 611, Little Rock, AR, 72205

Phone: 501-686-7335

Fax: 501-526-4618

Email: epeterson@uams.edu

Number of text pages: 27

Number of tables: 0

Number of figures: 6

Number of references: 25

Abstract word count: 218

Introduction word count: 799

Discussion word count: 1701

Abstract

Methamphetamine (METH) continues to be amongst the most addictive and abused drugs in the US. Unfortunately, there are currently no FDA approved pharmacological treatments for METH use disorder. We have previously explored the use of Adeno-Associated Viral (AAV) mediated gene transfer of an anti-METH monoclonal antibody. Here, we advance our approach by generating a novel anti-METH scFv-Fc fusion construct (termed 7F9-Fc), packaged into AAV serotype 8 vector (called AAV-scFv-Fc), and tested in vivo and ex vivo. A range of doses (1×10^{10}, 1×10^{11}, and 1×10^{12} vector copies(vc)/mouse) were administered to mice, eliciting a dose-dependent expression of 7F9-Fc in serum with peak circulating concentrations of 48, 1785, and 3,831 µg/ml, respectively. Expressed 7F9-Fc exhibited high affinity METH binding, IC_{50} = 17 nM. Between days 21 and 35 after vector administration, at both 1×10^{11} vc/mouse and 1×10^{12} vc/mouse doses, the 7F9-Fc gene therapy significantly decreased the potency of METH in locomotor assays. On day 116 post AAV administration, mice expressing 7F9-Fc sequestered over 2.5 times more METH in the serum than vehicle-treated mice, and METH concentrations in the brain were reduced by 1.2 times the value for vehicle mice. These data suggest that an AAV-delivered anti-METH Fc fusion antibody could be utilized to persistently reduce concentrations of METH in the CNS.

Significance Statement

In this manuscript, we describe the testing of a novel anti-METH scFv-Fc fusion protein delivered in mice using gene therapy. The results suggest that the gene therapy delivery system can lead to the production of significant antibody concentrations which mitigated METH's psychostimulant effects in mice over an extended time period.

Introduction

Methamphetamine (METH) use disorder (MUD) has been increasing yearly since at least 2008 and its use as an illicit drug is second only to opioid abuse (Winkelman *et al.*, 2018; Artigiani *et al.*, 2019). Recovery from MUD is difficult, with rates of relapse over 60% within the first year of abstinence (Brecht and Herbeck, 2014). One pharmacological approach to aid in the recovery from MUD is to use anti-METH monoclonal antibodies (mAbs) to block or blunt METH effects. Rather than targeting the sites of METH's action in the brain, these antibodies could act as pharmacokinetic antagonists, sequestering METH in the blood and reducing the amount reaching the brain (McMillan *et al.*, 2002). MAb therapy could be used in conjunction with behavioral therapies. For example, if METH use occurs during the course of therapy, anti-METH mAbs, by either preventing or greatly decreasing the direct effects of METH, could improve the chances of patients continuing with MUD therapy rather than relapsing

Delivery of the mAb by gene therapy could greatly extend the duration of action, reduce dosing frequencies, and reduce the impact of potential noncompliance issues. Adeno-associated viruses (AAV) are commonly used as gene therapy vectors because they are non-pathogenic viruses that can deliver up to 4.5 kilobases of DNA to host tissues (Zolotukhin, 2005). Previous studies in mice have shown that a single dose of AAV, delivering DNA encoding an entire mAb sequence, reaches maximal expression of mAb in 3-4 weeks and expression persists for at least 8 months (Hicks *et al.*, 2012; Rosenberg *et al.*, 2012, 2013; Hay *et al.*, 2018). Hicks *et al.* (2012) showed that an anti-nicotine AAV based mAb therapy elicited over 4-fold greater circulating concentrations of high affinity mAbs with one injection compared to an anti-nicotine vaccine in rodents, which generated variable amounts of polyclonal antibodies and required two additional booster doses. These previous studies suggest that, in comparison to a METH vaccine, an optimized anti-METH gene therapy should be able to sequester greater levels of METH in the serum after only one injection without the need for boosters.

JPET Fast Forward. Published on April 3, 2020 as DOI: 10.1124/jpet.119.261180
This article has not been copyedited and formatted. The final version may differ from this version.

Other laboratories have successfully developed AAV-based mAb therapies against various drugs of abuse (Hicks *et al.*, 2012; Rosenberg *et al.*, 2012). A full IgG antibody sequence can fit into an AAV capsid, but requires post-translational autocleavage of the heavy and light chains of the IgG antibody before dimerizing back together through disulfide bonds (Fang *et al.*, 2005; Ho *et al.*, 2013). In contrast, we have previously reported the design and testing of a single chain variable fragment (scFv7F9), which consists of the variable regions of an IgG connected by a 15 amino acid linker (Hay *et al.*, 2018). ScFv7F9 binds with high affinity to METH (K_D = 6.2 nM) and to the active metabolite amphetamine, with lower affinity (IC_{50} = 8 μM) (Nanaware-Kharade *et al.*, 2015). The short half-life of scFvs, which is approximately 60 min due to high clearance rate, limits the circulating concentrations of anti-METH antibodies in mice. (Nanaware-Kharade *et al.*, 2015; Reichard *et al.*, 2016; Hay *et al.*, 2018).

An improvement in scFv therapeutic antibody properties was implemented using an scFv-Fc fusion protein.The scFv-Fc fusion possesses much of the simplicity of an scFv being one amino acid sequence, but has an increased half-life of about 108 hours (Unverdorben *et al.*, 2016). An scFv-Fc fusion consists of an scFv, connected to the C_{H2} and C_{H3} regions of an IgG constant region (Repp *et al.*, 2011), which can then create a homodimer with another copy of itself. An scFv-Fc fusion has the potential to avoid the more complex post-translational processing that is necessary for IgG assembly, with a much longer half-life than an scFv. ScFv-Fc fusions are reported to have serum half-lives of 104-112 hrs compared to the 218-222 hrs of a full IgG antibody (Unverdorben *et al.*, 2016). This lead to our hypothesis that the inclusion of the Fc region from an IgG antibody, forming an scFv-Fc fusion antibody against METH, would yield high circulating concentrations. These high concentrations of the novel antibody should sequester greater concentrations of METH in the circulation and significantly reduce the psychostimulant effects of METH in mice over significant time periods.

In this study, we report a newly designed anti-METH scFv-Fc biotherapeutic (7F9-Fc) packaged into an AAV8 viral vector. We report a dose-dependent relationship between the

AAV8 viral vector copies administered and the concentration of 7F9-Fc in the serum of mice. A 1×10^{12} vc/mouse dose of AAV-7F9-Fc results in antibody circulating concentrations in the mg/ml range over an 8-month period. Studies of locomotor activity showed that METH psychostimulant effects were decreased in potency in mice expressing AAV-7F9-FC, and biodistribution studies showed that there were significant increases in the METH brain:serum ratio at 30 min after a 3.1 mg/kg METH dose.

JPET Fast Forward. Published on April 3, 2020 as DOI: 10.1124/jpet.119.261180
This article has not been copyedited and formatted. The final version may differ from this version.

Methods and Methods

Animal usage

Adult (3-4 weeks old), male, BALB/c mice were obtained from Charles River Laboratories (Raleigh, NC). Mice were housed 3-6 mice per cage in a light-controlled environment (12 hr light/dark cycle). Mice were allowed food and water *ad libitum*. Mice were randomly placed into groups for all experimental studies. The use of mice for experiments was approved by the Institutional Care and Use Committee of the Universities of Arkansas for Medical Sciences and was in accordance with the "Guide for the Care and Use of Laboratory Animals" (National Research Council 2011).

Drugs and Reagents

All S-methamphetamine (METH) used, both unlabeled and tritium-labeled, was obtained as an HCl salt from the National Institute of Drug Abuse (Bethesda, MD). METH was weighed as the salt version and dissolved in 1x PBS. Unless otherwise stated, reagents and other materials were purchased from ThermoFisher Scientific (Waltham, MA). Isolation and purification of plasmids and proteins were performed using Qiagen kits (Valencia, CA). METH ampules were bought for standard curve samples and quality control samples from Cerilliant (Round Rock, TX). DNA digestion enzymes were purchased from New England Biolabs (Ipswich, MA).

Design and generation of 7F9-Fc plasmids and AAV8 capsids

The scFv-Fc fusion construct, 7F9-Fc, was derived from an anti-METH mAb previously generated, consisting of scFv7F9 and C_{H2} and C_{H3} regions (Peterson *et al.*, 2008). The sequences were capped with a 6-histidine tail (6HIS) at the carboxy terminus, and expressed with a cleavable, signal secretion sequence (hambp) to ensure correct folding and routing

through the cellular secretory pathway (Tyagi *et al.*, 2002). Plasmids were cloned into cassettes with a human α-1 anti-trypsin promoter (HAAT) prior to the hambp sequence. The cassette structure is shown in Figure 1A.

The sequences containing 7F9-Fc cDNA, were custom synthesized and ligated into pUC57 (GenScript). Plasmids containing the antibody sequences were transformed into Invitrogen Top10F competent cells (Thermo #C303003) as per manufacturer recommendations and sequences were confirmed by at the University of Arkansas for Medical Sciences DNA Sequencing Core Facility. Plasmids were transformed into Top10F cells and colonies of transformed cells were grown on agar plates containing 50 μg/ml ampicillin. Colonies were selected and added to baffled flasks containing 1 liter of LB with 50 μg/ml ampicillin. Cultures were grown overnight with shaking at 225 rpm at 37^{o} C. Qiagen Endotoxin-free Mega (#12381) plasmid kits were used to isolate the plasmid DNA. DNA purity and concentrations were determined by $UV_{260/280}$ spectrophotometry and gel electrophoresis via plasmid digestions using the digestion enzymes EcoRI and XhoI (New England Biolabs # R3101S and R0146S respectively).

Plasmids containing the construct DNA were shipped to the Children's Hospital of Philadelphia to be ligated into the expression vector, AAV–hAAT-F.IX as described in Margaritis *et al.*, (2004). These ligated expression vectors were then sent to SAB Tech (Philadelphia, Pennsylvania), who employs a helper virus-free, triple plasmid transfection method for AAV8 vector production and packaging into viral vectors.

Determining titers and duration of expression

Four to six mice per group were administered 1 x 10^{10}, 1 x 10^{11}, or 1 x 10^{12} vector copies (vc) of AAV-7F9-Fc per mouse or equal volumes of 5% sorbitol (w/v) in 1X PBS for the vehicle group via tail vein. Tail snips were performed every two to four weeks to collect blood samples

from each mouse (Hay *et al.*, 2018). The serum was isolated from the red blood cells via centrifugation (12,000 rcf for 10 min) and stored at -80^{O} C.

Functional, sandwich ELISAs were performed as previously described to determine the circulating concentrations of 7F9-Fc at each time point (Hay *et al.*, 2018). Briefly, the serum samples were diluted 1:5,000, and a HRP anti-His tag antibody (Biolegend, #652504) diluted 1:1000 in Superblock (Thermo #37515) was used as the secondary detection antibody. 1-Step Ultra TMB-ELISA (Thermo #34029) was utilized to react with the HRP on the secondary antibodies. Wells were measured for light absorption at 480 nm on a Biotek HT Synergy plate reader. Concentrations of the anti-METH antibodies were interpolated from a standard curve of purified scFv7F9 protein (Reichard *et al.*, 2016).

Biocharacterization

Western blots were performed as previously described to confirm the relative size of the expressed 7F9-Fc constructs (Hay *et al.*, 2018). Briefly, serum samples collected 22 days post-AAV administration were pooled from each AAV dose group and diluted 1:13 before applying to the Western blot membranes. Serum pooled from vehicle mice on day 22 was used as a negative control to show mice not given the AAV-7F9-Fc vectors did not express 7F9-Fc protein. Purified scFv7F9 protein with a 6His tag was used as a positive control (Reichard *et al.*, 2016). The Western blot membranes were stained with HRP anti-His tag antibody (Biolegend, #652504) diluted 1:2,000 in 0.5% (w/v) BSA. Membranes were developed using Pierce ECL Western Blotting Substrate (Thermo #32106). Due to the use of a standard curve in the ELISA assays to precisely interpolate expression level, Western blot bands were not quantified.

Determination of AAV-7F9-Fc antibody *ex vivo* function

Radioimmunoassays were performed as previously described to determine the IC_{50} values for METH binding to 7F9-Fc (Owens *et al.*, 1988; Peterson *et al.*, 2007). Briefly, 10 μl of

serum samples or METH standards in serum (concentrations from 0.03 nM to 500 nM) were added to duplicate polypropylene tubes containing: 20 μl of magnetic MagnaBind protein G beads (Thermo #213498), 100 μl of 500 dpm/μl ^{3}H-METH, and 100 μl of blank serum diluted 1:1000. After 18 hrs of gentle mixing at 4^{O} C, the tubes were placed over magnets for six min and the supernatant removed. The magnetic bead/antibody complexes were suspended in 2 ml ScintiVerse BD Cocktail (Thermo #163431). Vials were vortexed for 10 sec before quantitation by a Tri-Carb 2910 TR scintillation counter. An "[Inhibitor] vs. normalized response -- Variable slope" model (Graphpad Prism 7.0d) was fit to the METH serum standard curve data points to determine the IC_{50} of each unknown serum sample.

Disposition of METH after AAV-7F9-Fc treatment

Mice given either 1 x 10^{12} vc/mouse 7F9-Fc therapy or vehicle were administered 3.1 mg/kg METH subcutaneously (sc). Thirty min later mice were sacrificed and brains and trunk blood were harvested. After clotting, blood samples were centrifuged at 12,000 rcf for 10 min and serum was transferred into new tubes. Brains were homogenized in 4 ml of mass spectrometry grade H_2O per gram of brain tissue.

A previously described extraction method for (3,4)-methylenedioxypyrovalerone was adapted for the extraction of METH and AMP in serum and brain tissue (Hambuchen *et al.*, 2017). Twenty-five microliters of each sample or standard was added to a 1.5 ml centrifuge tube. A volume of 125 µl ice-cold 30 ng/ml methamphetamine-D5 (internal standard) in acetonitrile was added prior to brief vortex mixing. After adding the internal standard solution to all samples and standards, the mixtures were vortex mixed for an additional 10 sec prior to incubation for 10 min at 4°C. Afterward, the mixture was centrifuged at 20,000 rcf (at 4°C) for 5 min, and the supernatant was transferred to another 1.5 ml tube for drying in a Zymark

TurboVap LV evaporator (SOTAX Corporation) under gentle nitrogen flow in a water bath at 40°C.

Dried samples and standards were reconstituted with 75 µl of 0.1% formic acid and vortex mixed for 20 s. After reconstitution, samples were centrifuged at 20,000 rcf (at 4°C) for 5 min, and 65 µl of supernatant was transferred to an autoinjector plate where 7.5 µl were injected onto an Acquity UPLC BEH C18 1.7 µm (2.1 i.d. x 100 mm) column (Waters Corp, Milford, MA) in an Acquity Ultra Performance Liquid Chromatography system connected to a Quattro Premier XE mass spectrometer (Waters Corp).

Analysis of unchanged METH concentrations in extracted samples were performed by a previously described liquid chromatography tandem mass spectrometry (LC/MS-MS) method (Hambuchen *et al.*, 2015). The lower and upper limit of quantification for METH and AMP was 1 and 1000 ng/ml, respectively. All predicted values for calibration and quality control standards were within ± 20% of the actual concentrations.

Locomotor activity assays in mice

Two separate AAV-7F9-Fc locomotor studies were performed, one with 1 x 10^{11} vc/mouse AAV8 (n=8 mice/group) and one with 1 x 10^{12} vc/mouse AAV8 (n=6 mice/group). The 1 x 10^{11} vc/mouse study was performed between days 11 and 50 post-AAV administration and the 1 x 10^{12} vc/mouse study was performed on the mice between days 21 and 37 post-AAV administration. Mice were given at least 21 days to achieve steady expression of 7F9-Fc in the serum before administering drug *sc*. Mice were placed into 27.31 x 27.31 x 20.32 cm chambers (Med Associates # ENV-510S). Chambers were equipped with IR-beam transmitter strips (Med Associates # ENV-256T) and receiver strips (Med Associates # ENV-256R) with 24 beams/strip to create a horizontal grid. Transmitter/reciever beams were in groups of 3, 0.5 cm apart, and 1.3 cm spacing between beam triplets. Each chamber was illuminated during recording. Movement was recorded when mice interrupted beams. The software default settings for

JPET Fast Forward. Published on April 3, 2020 as DOI: 10.1124/jpet.119.261180
This article has not been copyedited and formatted. The final version may differ from this version.

movement were used. Food and water were not available while the mice were in the chambers. Mice were allowed to equilibrate to their surroundings for 90 min before being administered PBS, METH or cocaine *sc*.

For the 1 x 10^{11} vc/mouse study, mice were administered Saline, 1, 3, 5, and 7 mg/kg METH, and 10 and 30 mg/kg cocaine sc with at least a 1 day for washout period between doses. A 10 mg/kg cocaine sc dose was initially used as a positive control, but this dose failed to elicit a large increase in locomotor activity over saline, so a 30 mg/kg cocaine sc dose was also administrered. For the 1 x 10^{12} vc/mouse study, mice were given 1.7, 3.1, and 9.4 mg/kg METH sc with at least a 1 day washout period in between doses. These doses were prepared as 1.0, 3.0 and 10 mg/kg METH respectively, but afterwards were validated by LC-MS/MS and found to be slightly different from the target doses. For testing days, drug stocks were prepared such that an injection volume of 100 µl would deliver the desired dose to a mouse based on the mean weight of the group. The weight variation between individuals was less than 6%. The corrected values were used for all data analysis.

After drug administration, mice were placed back into their beam break boxes. Recording started once the mouse was placed in the box. Mouse activity was recorded for two hrs post injection. Afterwards, mice were placed back into their home cages. There was at least a two-day washout period between testing sessions. Activity was recorded as distance in cm, and was reported as the total distance traveled over 90 min post-administration of METH.

Statistical analyses

GraphPad Prism (version 7.0d, GraphPad Software, Inc.) was used to analyze all data. In order to determine appropriate n values before each study power analyses were performed using the http://clincalc.com/Stats/SampleSize.aspx website with power set to 0.8 and $\alpha = 0.05$. No outliers were identified in the data (Grubb's outlier test, $\alpha = 0.05$). Shapiro-Wilk normalcy tests were used to confirm data was normally distributed. The resulting data from the

METH biodistribution study analyzed via 1-tailed, unpaired t-tests. Unless otherwise noted, significance was determined at $p < 0.05$ and denoted with an asterisk.

For the 1 x 10^{12} vc/mouse dose locomotor results, the comparisons of the peak circulating concentrations of the construct between the different doses of AAV were tested with a one-way ANOVA using a Holm-Sidak post-hoc multiple comparison test when a significant difference was found between groups. After statistical significance was observed in the interaction between METH dose and AAV therapy for the locomotor assays with a two-way ANOVA simple main effect tests with a Holm-Sidak correction were performed to further asses interaction. Holm-Sidak multiple comparisons tests were also performed to compare effects of METH doses to saline doses. Data are reported as percent saline.

The locomotor activity results for the 1 x 10^{11} vc/mouse dose used a different set of analyses. The results were normalized by setting the smallest mean in each data set as 0% and the largest data set as 100%. Then a nonlinear regression model using an "[Agonist] vs. normalized response" equation was used to determine the EC_{50}'s of METH for mice given the AAV-7F9-Fc therapy and mice given vehicle. To show there was no difference in the efficacy of METH between treatment groups, the AUC's of each individual mouse were determined, and an unpaired t-test was performed. Data are reported as percent saline.

JPET Fast Forward. Published on April 3, 2020 as DOI: 10.1124/jpet.119.261180
This article has not been copyedited and formatted. The final version may differ from this version.

Results

Determining optimal AAV dose for 7F9-Fc serum expression

A dose-dependent relationship was observed in Figure 2A between the dose of AAV-7F9-Fc administered and the circulating concentration of anti-METH antibodies. Over the observed 170-day period, the mice administered 1 x 10^{10} vc/mouse peaked at 48 µg/ml, those administered 1 x 10^{11} vc/mouse peaked at 1,785 µg/ml, and those administered 1 x 10^{12} vc/mouse peaked at 3,831 µg/ml. A 1-way ANOVA of the peak values yielded significant variation between groups $F(2, 12) = 2.058$, $p<0.0001$. Tukey post-hoc tests showed there were significant differences in expression between each of the observed peak circulating concentrations ($p<0.05$).

Confirmation of Construct Size

Serum samples collected from mice on day 22 post-AAV administration were pooled by AAV dose (vehicle, 1 x 10^{10}, 1 x 10^{11}, or 1 x 10^{12} vc/mouse). The 7F9-Fc protein monomers were calculated to be 61.6 kDa. The intact monomeric 7F9-Fc bands appeared at the expected molecular size (60 kDa, Figure 2B). As observed in Figure 2B, the 7F9-Fc bands appear to increase in intensity with increasing AAV dose, but the band for the lowest concentration is not detectable. This is likely due to the very low 7F9-Fc concentration of the 1 x 10^{10} dose reported by ELISA in Figure 2A.

Affinity

Pooled serum samples from mice expressing 7F9-Fc collected 22 days after AAV administration showed the IC_{50} value for 7F9-Fc was 17 nM, while the mAb7F9 IC_{50} value was of 32 nM (Figure 3).

JPET Fast Forward. Published on April 3, 2020 as DOI: 10.1124/jpet.119.261180
This article has not been copyedited and formatted. The final version may differ from this version.

Duration of anti-METH antibody expression in mice

We selected the highest 1 x 10^{12} vc/mouse dose of AAV-7F9-Fc for further studies. An additional mouse cohort administered this dose to determine the longevity of 7F9-Fc expression in vivo over an ~8-month observation period. As can be observed in Figure 4, the mice expressed 7F9-Fc anti-METH antibodies for at least 239 days after a single AAV administration. During the observation period, the mice exhibited an average circulating concentration of 2,116 ± 1,543 µg/ml, with a peak of 5,228 ± 1,637 µg/ml on day 63 post-AAV administration.

Locomotor studies

At the 1 x 10^{12} vc/mouse dose, the AAV-7F9-Fc therapy decreased the psychostimulant effects of METH at 3.1 and 9.4 mg/kg METH *sc* doses (Figure 5A) as compared to vehicle mice. A two-way ANOVA on the total distance traveled over a 90 min period revealed a statistically significant main effect of whether the therapy was administered ($F(1, 8) = 20.03$), a statistically significant main effect of the METH dose ($F(4, 32) = 9.384$), and the interaction between METH dose and AAV therapy was also significant ($F(4, 32) = 5.114$. A Holm-Sidak post-hoc test revealed significant difference between vehicle mice and mice treated with the AAV-7F9-Fc therapy at the 3.1 and 9.4 mg/kg METH *sc* doses, and also showed that there was no statistically significant difference in total distrance traveled between the METH doses and the saline doses in the mice treated with the AAV-7F9-Fc therapy. In all experimental groups, administration of saline had no effects on mouse behavior, and locomotor activity remained low for all subjects.

There was nearly a 2-fold shift to the right in the ED_{50} of METH for the mice administered 1 x 10^{11} vc/mouse of the AAV-7F9-Fc therapy (ED_{50}=3.2 mg/kg) compared to the vehicle mice (ED_{50} =1.7) mg/kg, as can seen in Figure 5B. The data observed in Figure 5B show that the AAV-7F9-Fc therapy can still reduce the potency of METH by nearly 2-fold at 48% of the average circulating 7F9-Fc concentrations resulting from the 1 x 10^{12} vc/mouse dose. There

was not a significant difference in the observed maximal effectiveness of METH between the two groups (p = 0.0678). These mice exhibited an average 7F9-Fc circulating concentration of 230 µg/ml before testing began (62% lower than the 1 x 10^{12} group).

Physiological efficacy

Four months post-administration of either AAV or vehicle, the same mice used in the locomotor assays were given 3.1 mg/kg METH sc. As can be observed in Figure 6A, mice treated with AAV-7F9-Fc accumulated significantly less, p=0.03, METH in their brains (2407 ng METH/g brain) than vehicle mice (2863 ng METH/g brain). This equates to a 1.2 fold decrease in METH concentration in the brains of the treated mice. In the serum (Figure 6B), the treated mice sequestered significantly more, p=0.0053, METH in their serum (828 ng METH/ml serum) than vehicle mice (324 ng METH/ml serum), which equates to a 2.5 increase in METH in the serum of the treated mice.

Mouse health

Similarly to our previously reported data with the same concentration of AAV, no lasting adverse effects of either AAV administration or of 7F9-Fc expression were observed as a result of the high AAV dose (Hay *et al.*, 2018).

JPET Fast Forward. Published on April 3, 2020 as DOI: 10.1124/jpet.119.261180
This article has not been copyedited and formatted. The final version may differ from this version.

Discussion

The purpose of this study was to design and test both in vivo and ex vivo, a long-lasting AAV-delivered anti-METH antibody therapy. The overarching hypothesis was that continuous expression of a high affinity anti-METH antibody with a long-lasting serum residence time could be a viable approach for creating medications to aid in treatment of METH use disorders. We have previously presented proof-of-concept data on expression of such an approach with an anti-METH mAb transgene (Hay *et al.*, 2018). Here, we wanted to increase the transgene expression and provide data on its functional capacity against METH effects. For this purpose, we engineered a single gene sequence based on a high affinity monoclonal antibody (mAb7F9) that could efficiently be packaged into AAV8 particles. By incorporating an Fc region into the construct, detectable expression lasted at least another month with average expression levels of 2,100 μg/ml. This produced thirty times greater concentrations than the first generation constructs, which was likely due to significantly reduced clearance of scFv-7F9-Fc (Hay *et al.*, 2018).

Three doses of the AAV-7F9-Fc therapy: 1 x 10^{10}, 1 x 10^{11}, and 1 x 10^{12} vc/mouse were used to determine dose-response effects on serum concentrations of expressed scFv-7F9-Fc. Because a significantly higher circulating concentration of our anti-METH construct at the 1 x 10^{12} vc/mouse dose was detected, we chose this dose to determine the potential upper limit of reduction of the pharmacological effects of METH. Future studies will be required to determine what dose of the AAV-7F9-Fc therapy provides the optimal circulating concentrations for the AAV dose given.

As can be observed in Figure 5A, locomotor activity following administration of the 9.4 mg/kg METH dose for the treated mice, while not significantly greater than activity observed after the saline doses, appears to be visually greater than the activity quantified after treatment with either of the two lower METH doses. While a more extensive panel of behavioral assays would be required to confirm, the data appear to suggest that the AAV-7F9-Fc treated mice are

beginning to exhibit psychostimulant effects of METH around the 9.4 mg/kg METH dose, compared to the vehicle mice beginning to exhibit the psychostimulant effects of METH between the 1.7 and 3.1 mg/kg METH doses. Using linear regressions, the treated mice required about 3.8 times more METH to exhibit the same level of activity at the 9.4 mg/kg METH *sc* dose. This indicates that the 1 x 10^{12} vc/mouse dose of AAV-7F9-Fc decreases the potency of METH nearly 4-fold.

To better understand the dose-effect relationship between 7F9-Fc circulating concentrations and psychostimulant effects of METH, a second locomotor assay was performed with mice administered 1 x 10^{11} AAV-7F9-Fc vc/mouse. We observed that both treated and vehicle mice exhibited a classic inverted "U" dose-reponse curve. We were unable to observe a descending limb in dose-effect curves in the 1 x 10^{12} vc/mouse locomotor study, as about half of the mice began exhibiting adverse METH effects at 16 mg/kg and the assay was terminated. Because descending limbs could be recorded for the 1 x 10^{11} AAV-7F9-Fc vc/mouse dose locomotor study, a different, more descriptive set of calculations could be performed to explain these results. This locomotor study also suggests that, while the AAV-7F9-Fc therapy can reduce the potency of METH, it might not be completely effective at reducing all of METH's adverse effects at extremely high doses (i.e., once the antibodies have exceeded full-occupancy). This is similar to other antagonists that can be surmounted with extremely high drug doses, such as naltrexone for opioid use disorders.

We acknowledge that the METH locomotor activity dose response curves in Figure 5 don't neatly match up above the 3 mg/kg METH sc doses. The mice administered 1 x 10^{11} vc/mouse of AAV-7F9-Fc were more active overall than the mice in the 1 x 10^{12} vc/mouse locomotor study. The two locomotor studies were performed over 2 years apart, but other variables were matched as closely as possible including the mouse vendor, the age of the mice when performing the studies, and the experimental setup. In an attempt to reduce baseline activity, the box habituation time was increased and additional saline sessions were run, but the

1 x 10^{11} vc/mouse mice continued to exhibit more activity than the 1 x 10^{12} vc/mouse mice. Nevertheless, the decreased locomotor effects of methamphetamine observed at doses above 3.0 mg/kg for control mice in Figure 5B (consistent with induction of motor stereotypy) were not observed for control mice in Figure 5A, even at a 3-fold higher dose. We can only attribute this to non-specific cohort effects. Despite this acknowledged cohort difference, a very consistent locomotor effect of 3.0 or 3.1 mg/kg METH was observed in both studies, where activity was increased to approximately 300% of saline control in vehicle mice. Importantly, the AAV-7F9-Fc therapy dose-dependently decreased these METH effects, to approximately 200% of saline control in the 1 x 10^{11} vc/mouse group and to approximately 100% of saline control in the 1 x 10^{12} vc/mouse group.

As previously noted, other groups (Hicks *et al.*, 2012; Rosenberg *et al.*, 2012, 2013) have successfully expressed full IgG antibodies using gene transfer. While this approach is viable, we hypothesized that a simpler approach might result in higher circulating concentrations due to less cellular processing. The scFv-Fc fusion construct can be expressed as a single continuous chain, which does not require post-translational cleavage steps for assembly (Unverdorben *et al.*, 2016). Further, scFv-Fc fusion constructs were previously shown to have similar half-lives compared to full IgG antibodies, primarily due to similar sizes and utilizing the FcRn pathway, which greatly increases the half-life of proteins (e.g. antibodies) beyond what would be predicted for proteins of their size (Ghetie *et al.*, 1996).

We also chose to utilize the IgG_2 subclass rather than the IgG_1 subclass as others have (Hicks *et al.*, 2012; Rosenberg *et al.*, 2012). The IgG_2 subclass has a similar affinity to the FcRn, but IgG_2 has a lower affinity for the Fc receptors on effector cells and is far less effective at activating complement (Vidarsson *et al.*, 2014), which is not needed in our treatment modality. These differences could translate to a decrease in undesirable systemic immune responses as a result of the expressed anti-METH antibodies.

Although, the variable region for both of the 7F9-Fc and mAb7F9 standard proteins is the same, the Fc regions of the protein are different, which perhaps could explain the difference in affinity (17 nM vs 32 nM). This pattern was observed by the scFv constructs of scFv7F9 showing an affinity to METH of 22 nM compared to an affinity of 48 nM of the purified standard (Hay *et al.*, 2018). This is the first time our group has compared the affinity of the 7F9-Fc construct to the original IgG mAb7F9 within the same assay. The overlapping locomotor effects in treated and untreated mice in response to the 10 and 30 mg/kg *sc* cocaine administrations in the 1 x 10^{11} vc/mouse locomotor study (Figure 5B) suggests that the AAV-7F9-Fc therapy is selective to METH. Further, the similarity in responses between treated and untreated mice to both cocaine doses may suggest that the AAV-7F9-Fc therapy does not affect central dopaminergic pathways which mediate locomotor effects of psychostimulants, or non-specifically alter drug metabolism. The AAV-7F9-Fc dose-dependent decreases in METH-elicited locomotor stimulation are therefore consistent with decreased METH concentrations in the CNS and increased METH sequestration in the serum, as demonstrated in Figure 6.

The data shown in Figure 6 indicate that 30 min post-METH administration, approximately T_{max} for METH in mice brain and serum (Magyar *et al.*, 2007), significantly greater concentrations of METH are being sequestered in the serum of the treated mice. When this study was performed (day 129) the antibody circulating concentration of 87 µg/ml resulted in a METH concentration of 827±279 ng/ml in the serum. This resulted in a METH:7F9-Fc molar ratio of 1,561:1 (5.54 mM METH and 3.55 µM 7F9-Fc), but even with this low antibody concentration, we observed sequestration of METH in the serum and reduction in brains of the treated mice compared to the vehicle mice. Had the assay been performed shortly after the mice had finished the locomotor assay with concentrations of about 600 µg/ml (data not shown), the reduction of METH in the brains would likely have been much greater. This dose of METH was selected to challenge the circulating antibodies and it shows that even after the antibody is surmounted, physiological efficacy can be observed.

In conclusion, our studies show the design, expression, and pre-clinical characterization of a high affinity, long duration of action anti-METH antibody-based gene therapy. The incorporation of the Fc region of the antibody fragment resulted in sustained circulating serum concentrations of over 2.1 mg/kg in mouse serum over a period of almost eight months. Biodistribution characterization suggests that the therapy was capable of sequestering METH in the serum and out of the brain. Data from behavioral assays suggest that this anti-METH gene therapy decreases the potency of METH to elicit locomotor stimulant effects by 2 to 4-fold, depending on the dose of AAV administered. Taken together, these initial studies suggest that a scFv-Fc based AAV therapy can decrease the potency the stimulant effects of METH by reducing the amount of METH able to enter the brain in mice.

Acknowledgements

We would like to thank Melinda Gunnell, Michael Berquist II, Madison Berg, and Robin Mulkey for their expert technical assistance.

Authorship contributions

Participated in research design: Hay, Peterson

Conducted experiments: Hay, Ewing, Hambuchen, Zintner, Small, Bolden

Contributed new reagents or analytic tools: Peterson, Owens, Fantegrossi, Margaritis

Performed data analysis: Hay, Hambuchen, Peterson

Wrote or contributed to the writing of the manuscript: Hay, Ewing, Hambuchen, Zintner, Small, Fantegrossi, Margaritis, Owens, Peterson

Financial disclosures

SMO has financial and fiduciary interests in InterveXion Therapeutics LLC, a biopharmaceutical company. The University of Arkansas for Medical Sciences has licensed intellectual property developed by SMO to InterveXion Therapeutics Therapeutics LLC.

References

Artigiani EE, Hsu MH, McCandlish D, and Wish ED (2019) *METHAMPHETAMINE A REGIONAL DRUG CRISIS*, National Drug Early Warning System, College Park, MD.

Brecht M-L, and Herbeck D (2014) Time to relapse following treatment for methamphetamine use: a long-term perspective on patterns and predictors. *Drug Alcohol Depend* **139**:18–25.

Fang J, Qian J-J, Yi S, Harding TC, Tu GH, VanRoey M, and Jooss K (2005) Stable antibody expression at therapeutic levels using the 2A peptide. *Nat Biotechnol* **23**:584–590.

Ghetie V, Hubbard JG, Kim JK, Tsen MF, Lee Y, and Ward ES (1996) Abnormally short serum half-lives of IgG in beta 2-microglobulin-deficient mice. *Eur J Immunol* **26**:690–696.

Hambuchen MD, Carroll FI, Rüedi-Bettschen D, Hendrickson HP, Hennings LJ, Blough BE, Brieaddy LE, Pidaparthi RR, and Owens SM (2015) Combining Active Immunization with Monoclonal Antibody Therapy To Facilitate Early Initiation of a Long-Acting Anti-Methamphetamine Antibody Response. *J Med Chem* **58**:4665–4677.

Hambuchen MD, Hendrickson HP, and Owens SM (2017) Chiral determination of 3,4-methylenedioxypyrovalerone enantiomers in rat serum. *Anal Methods Adv Methods Appl* **9**:609–617.

Hay CE, Gonzalez GA, Ewing LE, Reichard EE, Hambuchen MD, Nanaware-Kharade N, Alam S, Bolden CT, Owens SM, Margaritis P, and Peterson EC (2018) Development and testing of AAV-delivered single-chain variable fragments for the treatment of methamphetamine abuse. *PloS One* **13**:e0200060.

Hicks MJ, Rosenberg JB, De BP, Pagovich OE, Young CN, Qiu J, Kaminsky SM, Hackett NR, Worgall S, Janda KD, Davisson RL, and Crystal RG (2012) AAV-directed persistent expression of a gene encoding anti-nicotine antibody for smoking cessation. *Sci Transl Med* **4**:140ra87-140ra87.

Ho SCL, Bardor M, Li B, Lee JJ, Song Z, Tong YW, Goh L-T, and Yang Y (2013) Comparison of internal ribosome entry site (IRES) and Furin-2A (F2A) for monoclonal antibody expression level and quality in CHO cells. *PloS One* **8**:e63247.

Magyar K, Szatmáry I, Szebeni G, and Lengyel J (2007) Pharmacokinetic studies of (-)-deprenyl and some of its metabolites in mouse. *J Neural Transm Suppl* 165–173.

Margaritis P, Arruda VR, Aljamali M, Camire RM, Schlachterman A, and High KA (2004) Novel therapeutic approach for hemophilia using gene delivery of an engineered secreted activated Factor VII. *J Clin Invest* **113**:1025–1031.

McMillan DE, Hardwick WC, Li M, and Owens SM (2002) Pharmacokinetic antagonism of (+)-methamphetamine discrimination by a low-affinity monoclonal anti-methamphetamine antibody. *Behav Pharmacol* **13**:465–473.

Nanaware-Kharade N, Thakkar S, Gonzalez GA, and Peterson EC (2015) A Nanotechnology-Based Platform for Extending the Pharmacokinetic and Binding Properties of Anti-methamphetamine Antibody Fragments. *Sci Rep* **5**:12060.

Owens SM, Zorbas M, Lattin DL, Gunnell M, and Polk M (1988) Antibodies against arylcyclohexylamines and their similarities in binding specificity with the phencyclidine receptor. *J Pharmacol Exp Ther* **246**:472–478.

Peterson EC, Gunnell M, Che Y, Goforth RL, Carroll FI, Henry R, Liu H, and Owens SM (2007) Using hapten design to discover therapeutic monoclonal antibodies for treating methamphetamine abuse. *J Pharmacol Exp Ther* **322**:30–39.

Peterson EC, Laurenzana EM, Atchley WT, Hendrickson HP, and Owens SM (2008) Development and preclinical testing of a high-affinity single-chain antibody against (+)-methamphetamine. *J Pharmacol Exp Ther* **325**:124–133.

Reichard EE, Nanaware-Kharade N, Gonzalez GA, Thakkar S, Owens SM, and Peterson EC (2016) PEGylation of a High-Affinity Anti-(+)Methamphetamine Single Chain Antibody Fragment Extends Functional Half-Life by Reducing Clearance. *Pharm Res* **33**:2954–2966.

Repp R, Kellner C, Muskulus A, Staudinger M, Nodehi SM, Glorius P, Akramiene D, Dechant M, Fey GH, van Berkel PHC, van de Winkel JGJ, Parren PWHI, Valerius T, Gramatzki M, and Peipp M (2011) Combined Fc-protein- and Fc-glyco-engineering of scFv-Fc fusion proteins synergistically enhances CD16a binding but does not further enhance NK-cell mediated ADCC. *J Immunol Methods* **373**:67–78.

Rosenberg JB, De BP, Hicks MJ, Janda KD, Kaminsky SM, Worgall S, and Crystal RG (2013) Suppression of nicotine-induced pathophysiology by an adenovirus hexon-based antinicotine vaccine. *Hum Gene Ther* **24**:595–603.

Rosenberg JB, Hicks MJ, De BP, Pagovich O, Frenk E, Janda KD, Wee S, Koob GF, Hackett NR, Kaminsky SM, Worgall S, Tignor N, Mezey JG, and Crystal RG (2012) AAVrh.10-mediated expression of an anti-cocaine antibody mediates persistent passive immunization that suppresses cocaine-induced behavior. *Hum Gene Ther* **23**:451–459.

Tyagi S, Salier J-P, and Lal SK (2002) The liver-specific human alpha(1)-microglobulin/bikunin precursor (AMBP) is capable of self-association. *Arch Biochem Biophys* **399**:66–72.

Unverdorben F, Richter F, Hutt M, Seifert O, Malinge P, Fischer N, and Kontermann RE (2016) Pharmacokinetic properties of IgG and various Fc fusion proteins in mice. *mAbs* **8**:120–128.

Vidarsson G, Dekkers G, and Rispens T (2014) IgG subclasses and allotypes: from structure to effector functions. *Front Immunol* **5**:520.

Winkelman TNA, Admon LK, Jennings L, Shippee ND, Richardson CR, and Bart G (2018) Evaluation of Amphetamine-Related Hospitalizations and Associated Clinical Outcomes and Costs in the United States. *JAMA Netw Open* **1**:e183758–e183758.

Zolotukhin S (2005) Production of recombinant adeno-associated virus vectors. *Hum Gene Ther* **16**:551–557.

Footnotes

The project described was supported by the National in Insitutes of Health (NIH): National Institute on Drug Abuse (NIDA): [R01-DA036600], the National Institute for General Medical Sciences (NIGMS):[T32-GM106999] and [R25-GM083297].

JPET Fast Forward. Published on April 3, 2020 as DOI: 10.1124/jpet.119.261180
This article has not been copyedited and formatted. The final version may differ from this version.

Legends for figures

Figure 1. Schematic of the scFv-Fc fusion construct. 1A shows a schematic of the different regions of the DNA sequence packaged into the AAV capsids. 1B shows the same sequences after being translated and folded; construct should form a homodimer before being secreted from the cell. HMM38, secretory signal; V_H, variable heavy region; Linker, amino acid linker; V_L, variable light region; C_{H2} and C_{H3}, constant regions 2 and 3 respectively; and 6His, 6-histidine tag for purification and identification.

Figure 2: A dose-dependent relationship exists between the dose of AAV given to mice and the level of expression of 7F9-Fc. A: Peak serum concentration of 7F9-Fc as determined by functional ELISA. (*, $p<0.05$) Data shown as mean ± SD, n = 8 per group. B: A western blot comparing the expressed size of construct (61 kDa) to that of a predecessor scFv standard of known size (23 kDa).

Figure 3: Comparison of IC_{50} values for METH between culture-produced mAb7F9 and mouse-expressed 7F9-Fc. The IC_{50} (nM) for all variants was estimated at 50% ^{3}H-METH bound (dotted line). Data shown as mean ± SD, n = 8 per group.

Figure 4: 7F9-Fc expression persists over 8 months. Mice given 1 x 10^{12} vector copies/mouse showed expression for at least 8 months, with an average expression of 2,100 ug/ml. Functional ELISAs were performed on mouse serum. Data given as mean ± SD, n = 6 per group.

Figure 5: 7F9-Fc significantly reduces the psychostimulant effects of METH. Two groups of mice, vehicle and mice given (A) 1 x 10^{12} vc AAV-7F9-Fc/mouse (B) 1 x 10^{11} vc AAV-7F9-Fc/mouse, were either administed saline or increasing doses of METH *sc*. The locomotor

activity measured as total distance traveled was recorded for 90 min. Comparison between AAV-7F9-Fc treated mice (#, $p < 0.05$). Comparison between vehicle and AAV-7F9-Fc mice (*, $p < 0.05$) Data are shown as mean ± SD, n= 6 (A) and n=8 (B) per group.

Figure 6: A comparison of METH brain and serum concentrations after a 3.1 mg/kg *sc* injection of METH. Two groups of mice, vehicle and mice given 1 x 10^{12} vc AAV-7F9-Fc/mouse, were administered 3.1 mg/kg METH sc. Thirty min after METH administration, mice were sacrificed and brains (A) and serum (B) were collected. METH concentrations were determine by LC/MS-MS (*, $p < 0.05$). Data points are shown as mean ± SD, n = 3-5 per group.

JPET Fast Forward. Published on April 3, 2020 as DOI: 10.1124/jpet.119.261180
This article has not been copyedited and formatted. The final version may differ from this version.

Figure 1

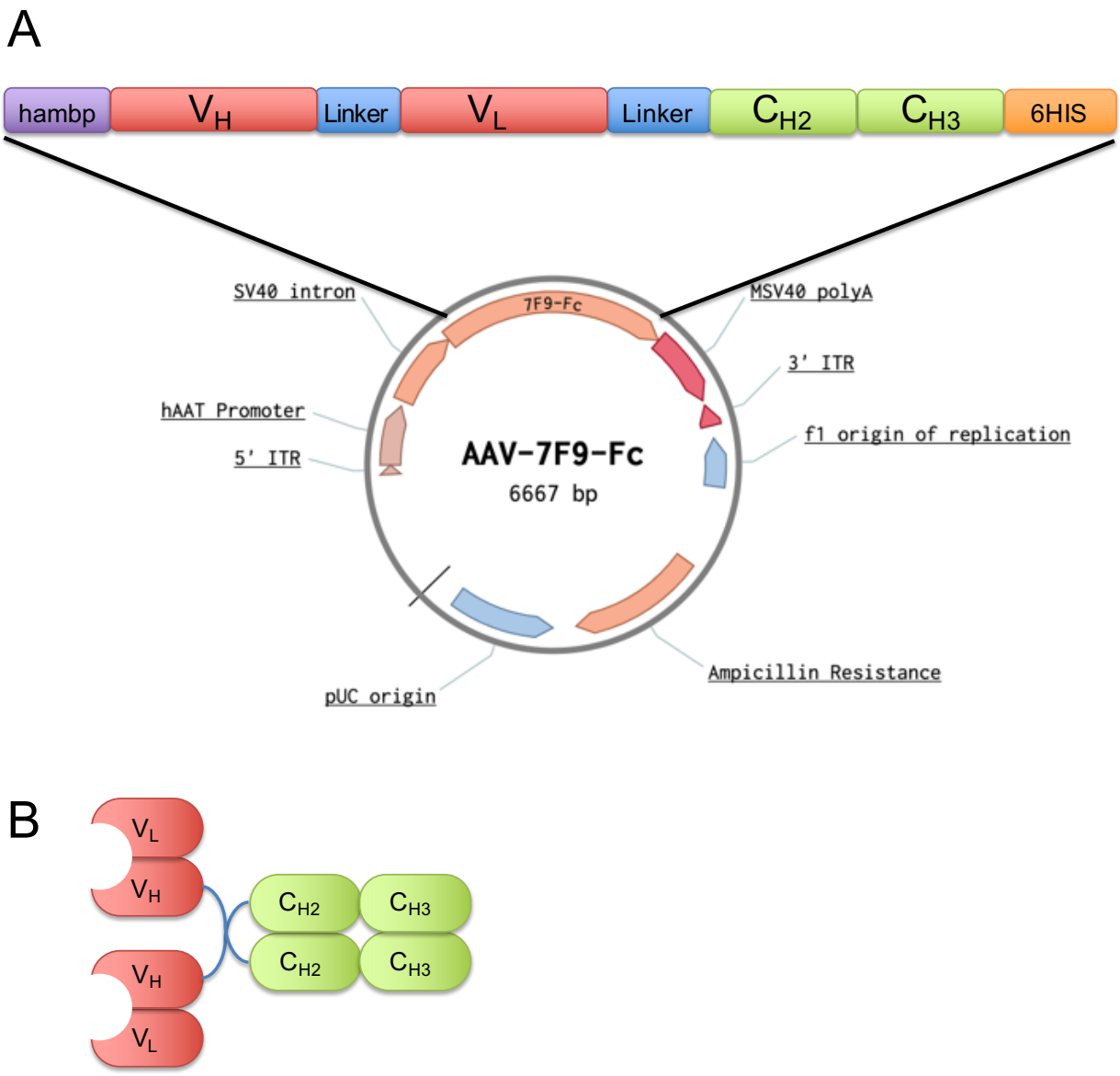

JPET Fast Forward. Published on April 3, 2020 as DOI: 10.1124/jpet.119.261180
This article has not been copyedited and formatted. The final version may differ from this version.

Figure 2

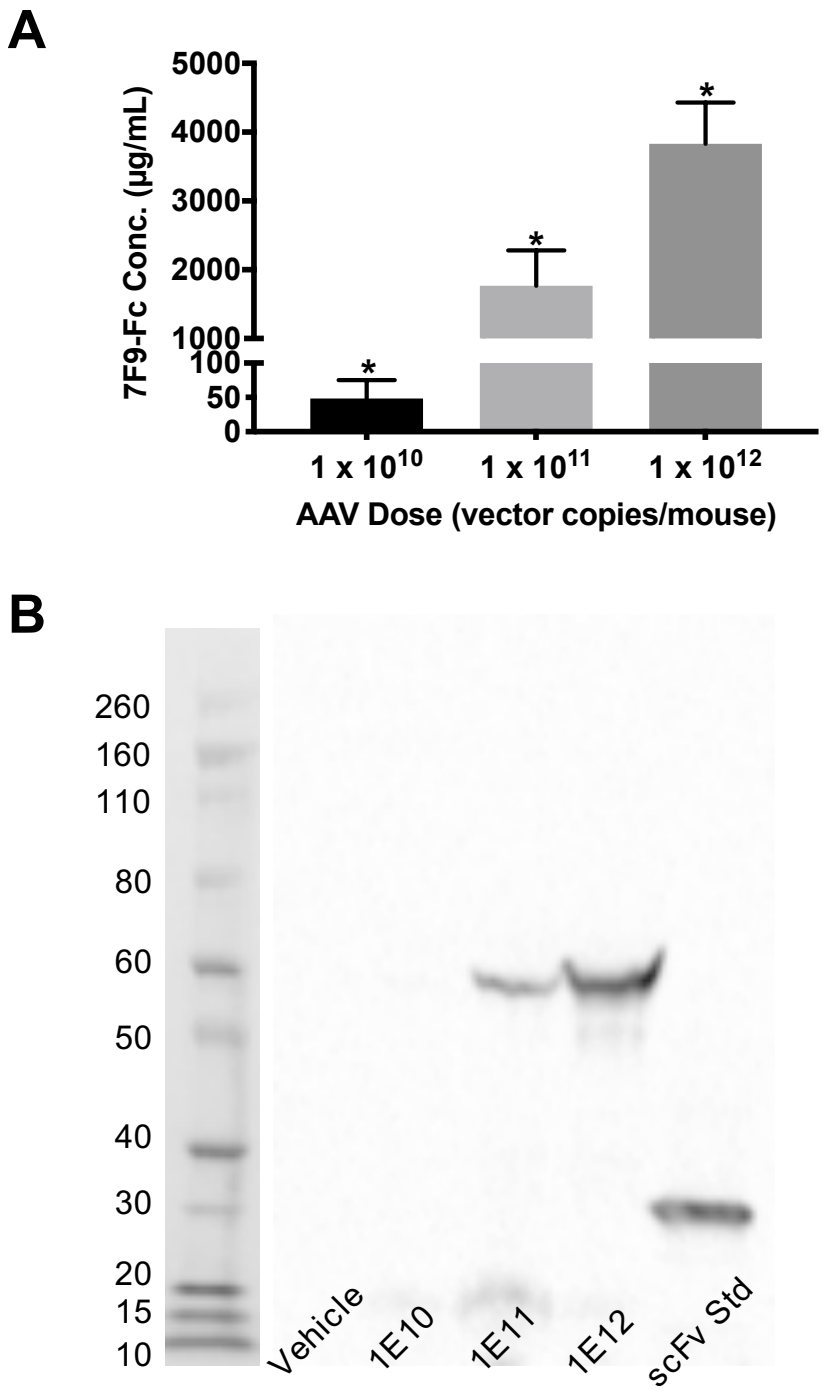

JPET Fast Forward. Published on April 3, 2020 as DOI: 10.1124/jpet.119.261180
This article has not been copyedited and formatted. The final version may differ from this version.

Figure 3

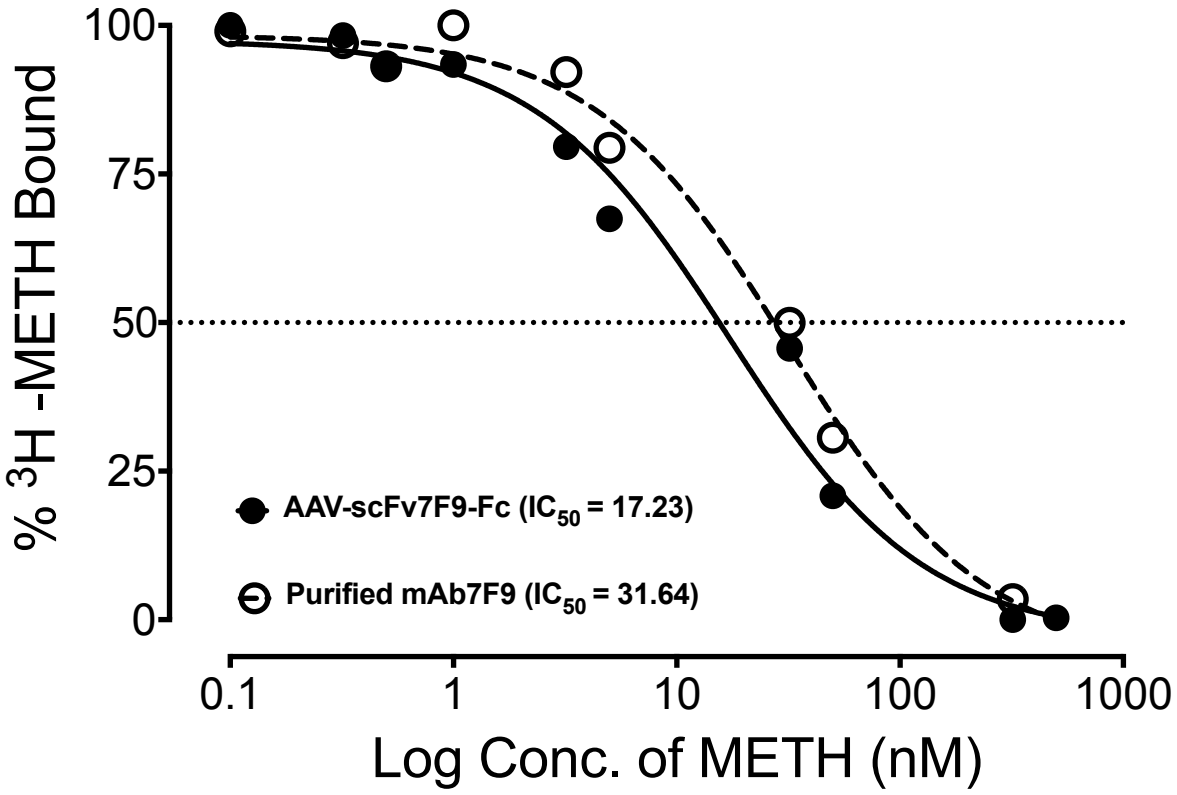

JPET Fast Forward. Published on April 3, 2020 as DOI: 10.1124/jpet.119.261180
This article has not been copyedited and formatted. The final version may differ from this version.

Figure 4

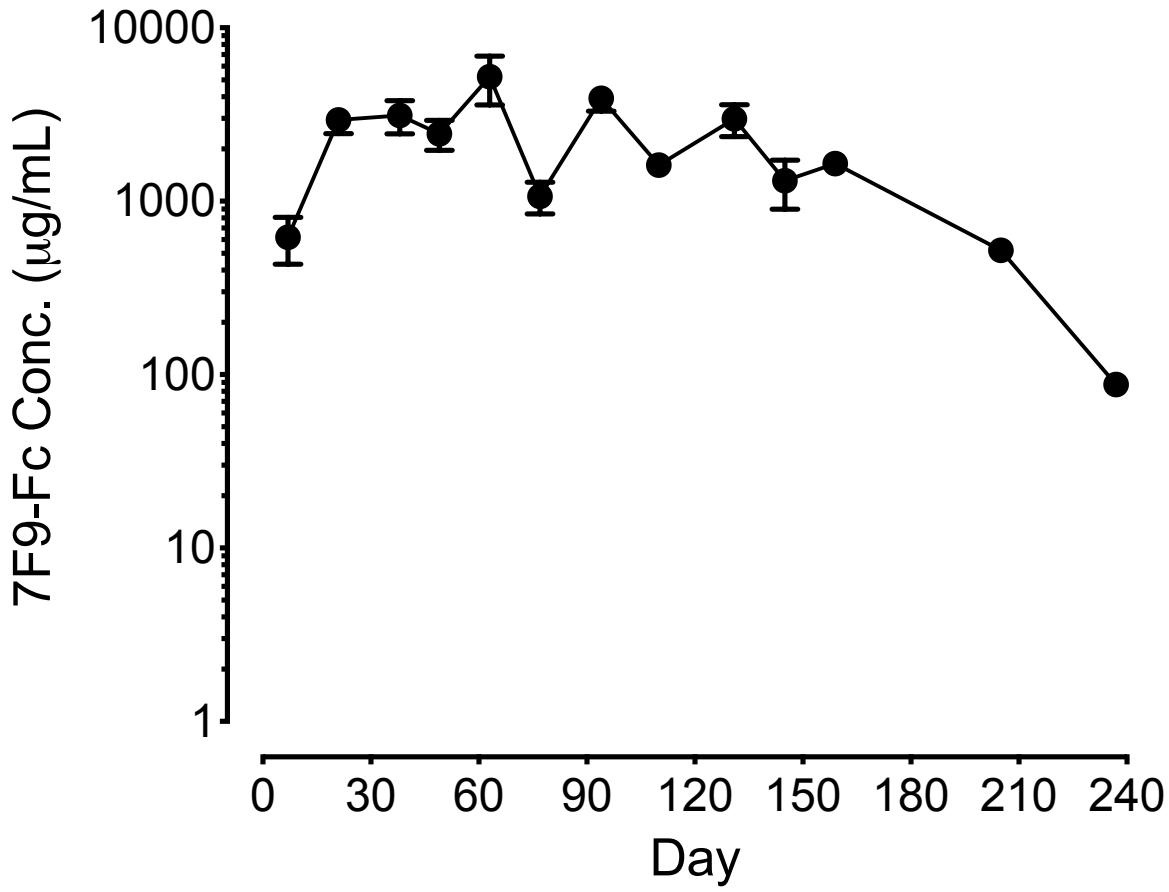

JPET Fast Forward. Published on April 3, 2020 as DOI: 10.1124/jpet.119.261180
This article has not been copyedited and formatted. The final version may differ from this version.

Figure 5

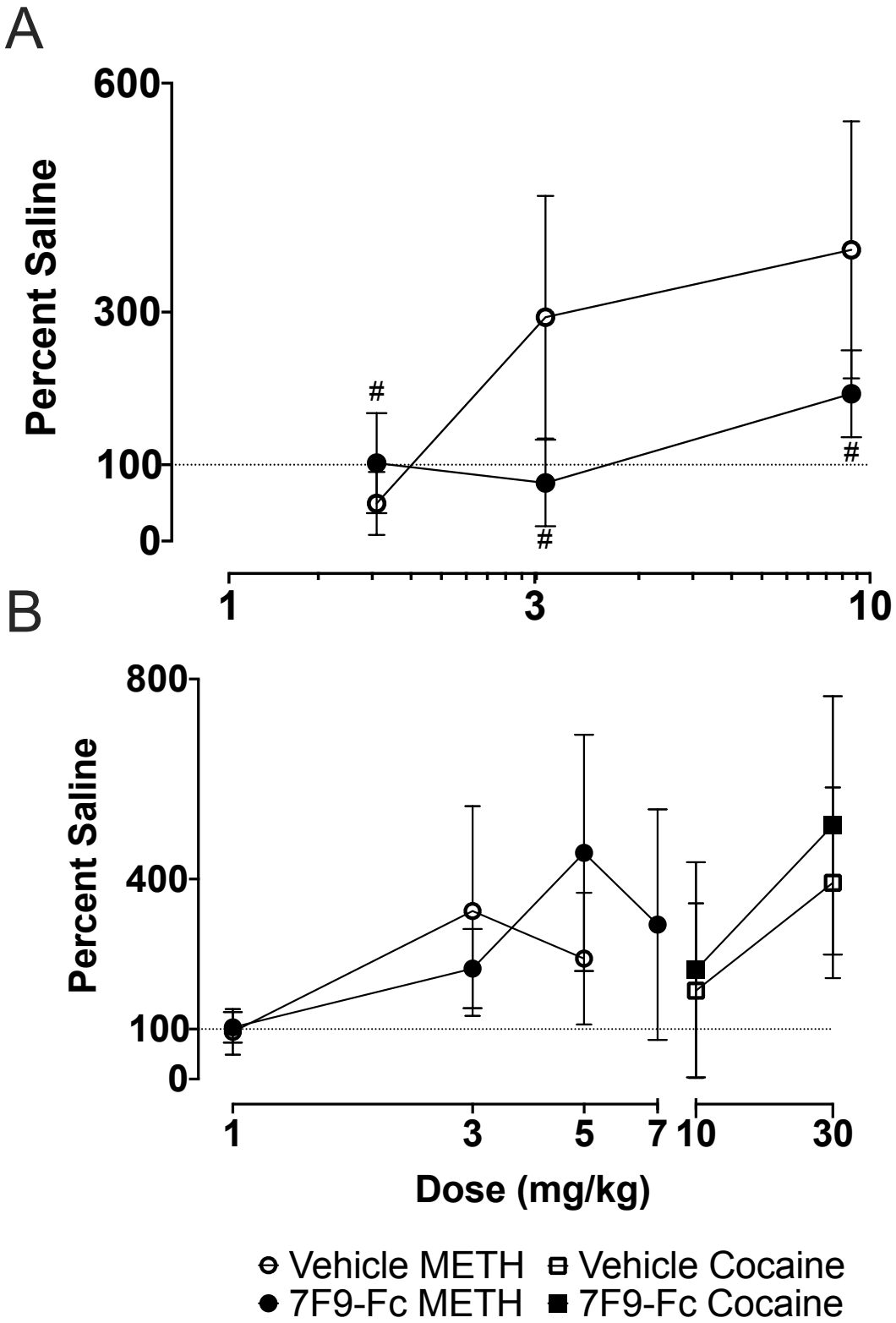

JPET Fast Forward. Published on April 3, 2020 as DOI: 10.1124/jpet.119.261180
This article has not been copyedited and formatted. The final version may differ from this version.

Figure 6